Cerebral Cortex, February 2020;30: 812–823

doi: 10.1093/cercor/bhz128
Advance Access Publication Date: 2 August 2019
Original Article

ORIGINAL ARTICLE

Language Without Speech: Segregating Distinct Circuits in the Human Brain

Theresa Finkl[1,*], Anja Hahne[1,*], Angela D. Friederici[2], Johannes Gerber[3], Dirk Mürbe[4] and Alfred Anwander[2,*]

[1]Saxonian Cochlear Implant Centre, Phoniatrics and Audiology, Faculty of Medicine, Technische Universität Dresden, Fetscherstraße 74, 01307 Dresden, Germany, [2]Department of Neuropsychology, Max Planck Institute for Human Cognitive and Brain Sciences, 04103 Leipzig, Germany, [3]Neuroradiology, Faculty of Medicine, Technische Universität Dresden, 01304 Dresden, Germany and [4]Department of Audiology and Phoniatrics, Charité—Universitätsmedizin, 10117 Berlin, Germany

Address correspondence to Theresa Finkl/Anja Hahne, Saxonian Cochlear Implant Centre, Phoniatrics and Audiology, Faculty of Medicine, Technische Universität Dresden, Fetscherstraße 74, 01307 Dresden, Germany. Phone: +49 351 458 7048, Email: anja.hahne@ukdd.de or Alfred Anwander, Max Planck Institute for Human Cognitive and Brain Sciences, Stephanstr. 1a, 04103 Leipzig, Germany. Phone: +49 341 9940-2626, Email: anwander@cbs.mpg.de
https://orcid.org/0000-0002-6495-858X https://orcid.org/0000-0002-4861-4808

Downloaded from https://academic.oup.com/cercor/article-abstract/30/2/812/5543064 by guest on 24 March 2020

Abstract

Language is a fundamental part of human cognition. The question of whether language is processed independently of speech, however, is still heavily discussed. The absence of speech in deaf signers offers the opportunity to disentangle language from speech in the human brain. Using probabilistic tractography, we compared brain structural connectivity of adult deaf signers who had learned sign language early in life to that of matched hearing controls. Quantitative comparison of the connectivity profiles revealed that the core language tracts did not differ between signers and controls, confirming that language is independent of speech. In contrast, pathways involved in the production and perception of speech displayed lower connectivity in deaf signers compared to hearing controls. These differences were located in tracts towards the left pre-supplementary motor area and the thalamus when seeding in Broca's area, and in ipsilateral parietal areas and the precuneus with seeds in left posterior temporal regions. Furthermore, the interhemispheric connectivity between the auditory cortices was lower in the deaf than in the hearing group, underlining the importance of the transcallosal connection for early auditory processes. The present results provide evidence for a functional segregation of the neural pathways for language and speech.

Key words: deaf, dMRI, DTI, language network, probabilistic tractography

Introduction

Language is a crucial part of human cognition and communication. The comprehension and production of spoken language requires the interplay between the core language network and the auditory input and motor output systems. Language itself, however, can be acquired independent of modality. This is the case in prelingually deaf individuals, who are either born deaf or lose their hearing before the acquisition of language (Smith et al. 1993). With vision-based sign language as their native language input, they develop language comparable to those of hearing people (Lillo-Martin and Gajewski 2014). Learning to read and write in later childhood consolidates language performance,

© The Author(s) 2019. Published by Oxford University Press.
This is an Open Access article distributed under the terms of the Creative Commons Attribution License (http://creativecommons.org/licenses/by/4.0/), which permits unrestricted reuse, distribution, and reproduction in any medium, provided the original work is properly cited.

though often at a lower level than in hearing non-signers. With additional training prelingually deaf people can also learn to visually decode spoken language primarily via lip reading, and to produce speech, but with clear limitations in the domains of phonation and articulation (Harris and Beech 1998). The unique situation of language without speech in deaf signers offers the possibility to disentangle the neural underpinnings of speech as an input–output system from those of the core language system. In the present study we achieved this by comparing the effect of auditory (oral) and visual (sign) language acquisition on the differential neuroplastic development of the respective structural brain networks.

The exact functional division of language and speech networks continues to be the subject of sustained scientific research. On a theoretical level (Berwick et al. 2013; Friederici et al. 2017), a core language system responsible for semantic and syntactic processes is distinguished from a sensory–motor interface system allowing communication via vocal production and auditory perception of speech. In sign language, this is achieved through the visual decoding of manual gestures and concomitant lip reading. At the neural network level, Broca's area in the left inferior frontal gyrus (IFG) and Wernicke's area in the left posterior temporal cortex extending to the inferior parietal lobule (IPL) are widely accepted as major nodes of the core language network (Price 2012; Hagoort, 2014). This core language network also supports semantic and syntactic processes in sign language (Emmorey et al. 2003; MacSweeney et al. 2002).

The frontal cortex and the temporal cortex also include brain areas relevant for speech production (ventral BA6 in the motor cortex) and for speech perception (Heschl's gyrus (HG) in the auditory cortex). These frontal and posterior temporal brain areas are connected by long-range white matter fiber tracts located dorsally and ventrally to the Sylvian fissure. We will discuss these in turn.

Dorsally, there are two distinguishable fiber pathways. The superior longitudinal/arcuate fasciculus (SLF/AF) connects the posterior portion of Broca's area (BA44) to posterior superior and middle temporal gyri (pSTG and pMTG) touching the IPL on its way (Catani et al. 2005; Anwander et al. 2007; Perani et al. 2011). This fiber tract has been demonstrated to be involved in the development and processing of complex syntactic structures (Friederici et al. 2006; Brauer et al. 2011; Skeide et al. 2016). Another part of the dorsal pathway running in parallel and also involving the SLF/AF targets the ventral precentral gyrus (ventral part of BA6: vBA6) and links speech motor areas to the auditory cortex (Catani et al. 2005; Perani et al. 2011). In a purely functional model Hickok and Poeppel (2007) proposed the dorsal processing stream to support sensory-motor processes, without however, further separating the dorsal stream into substreams. The presently available evidence suggests that there are two dorsal white matter fiber tracts and that the sensory-motor function should be related to the pathway targeting vBA6 (Saur et al. 2008). In an intracranial recording study, it has been shown that BA44 is activated prior to vBA6 during speech production, supporting the view that vBA6 is involved in the articulation of speech following the planning and initiation phase subserved by BA44 (Flinker et al. 2015). These two functionally distinct regions also exhibit differential functional connectivities: the ventral part of BA44 displays connections with language-relevant areas in the temporal and parietal cortex, while vBA6 is linked to input/output-related areas such as the pSTG and the face area in the central and postcentral gyrus responsible for tongue and lip movements (Zhang et al. 2017).

Another fiber tract involved in speaking is the frontal aslant tract (FAT). It connects vBA6 and BA44 as the most posterior parts of what is sometimes called "Broca's territory" (extending from BA44 frontally to BA45 and BA47) with the pre-supplementary motor area (preSMA) and SMA (Catani et al. 2013). This connection is essential for the articulation of words and forms part of the loop between frontal regions such as vBA6 and BA44, the basal ganglia, and the thalamus (Tha; for a review see Dick et al. 2019). It is important to note the FAT's differentiation between vBA6 and BA44 as well as between preSMA and SMA. Together with the cerebellum, these pathways convey information for the finely-tuned activity of the articulatory muscles necessary to produce comprehensible speech, which also implies their participation in the auditory feedback loop during speaking (Petacchi et al. 2005). Little is known about the neural basis for production of facial expressions during sign language production, although mouthing plays a crucial role. In German Sign Language (GSL), for example, the words "brother" and "sister" are performed with the same manual gesture, but different lip patterns. This makes it likely that pathways to vBA6 known to be relevant for speaking may also be relevant for signing.

Ventral to the Sylvian fissure, there are two main fiber tracts connecting the ventral part of the anterior portion of the IFG to the temporal cortex: the uncinate fasciculus and the inferior fronto-occipital fasciculus. Additionally, the inferior longitudinal and the middle longitudinal fasciculus extend posteriorly from the temporal pole. Functionally, these fiber tracts are attributed mainly to the processing of semantic information, but they have also been described in studies on emotion and cognitive control (for a review see Bajada et al. 2015). Among these, the most relevant tract for language processing is the inferior fronto-occipital fasciculus, which has been described to support semantic processes (Saur et al. 2008).

While semantic and syntactic processes are mainly subserved by this left-dominant network, there is increasing evidence that prosodic features of spoken language are processed in a right-dominant network (Sammler et al. 2015; Sammler et al. 2018). The interplay between the left and the right hemisphere during auditory language processing has been demonstrated in patients with lesions in the corpus callosum (CC; Friederici et al. 2007). This hemispheric dissociation between a system for semantic and syntactic processing in the left hemisphere and a system for processing prosodic information in the right hemisphere has also been discovered in sign language, where semantic and syntactic tasks activate the typical left-lateralized language regions (MacSweeney et al. 2002; Emmorey et al. 2003). Prosody in sign language is transmitted via trunk and head posture as well as via facial expression (Sandler 2012) and its interpretation has been shown to activate predominantly right-hemispheric inferior frontal and superior temporal regions. Studies reporting recruitment of the classic fronto-temporal network in both spoken and signed language (MacSweeney et al. 2002; Leonard et al. 2012) further support the concept of modality-independence of the language network. These neuroscientific findings fit well into the concept of a domain-independent language system, and is aligned with the finding that spoken and signed languages exhibit similar linguistic characteristics such as recursive rule application and hierarchical structures (Lillo-Martin and Gajewski 2014).

Before spoken language can be understood, the speech signal has to be pre-processed by the hearer's bihemispheric auditory

Downloaded from https://academic.oup.com/cercor/article-abstract/30/2/812/5543064 by guest on 24 March 2020

system, requiring interhemispheric fiber bundles that support a direct exchange of information between the two hemispheres. Strong connections exist within the temporal cortex (Upadhyay et al. 2008), but also to the auditory cortex in the opposite hemisphere via commissural fibers through the presplenial and splenial part of the CC (Huang et al. 2005; Chao et al. 2009). These connections subserve the rapid interhemispheric transfer of auditory speech signals within the perceptual system and thus pave the way for successful comprehension of speech. This, in turn, is substantially influenced by auditory attention, employing mid-temporal as well as mainly right-hemispheric superior parietal and frontal areas (Zatorre et al. 1999).

Before sign language can be understood, visual information has to be processed in the visual system. Therefore, differences in speech networks between deaf and hearing participants are likely and have previously been investigated functionally and with regard to gray matter structural alterations. In a pioneering brain imaging study, Finney et al. (2001) revealed a partial takeover of auditory areas by the visual system in profoundly deaf individuals. Brain plasticity is also possible in the white matter, as indicated by structural magnetic resonance imaging (MRI) studies showing short-term as well as long-term learning-induced cortical changes in both gray and white matter (Draganski et al. 2004; Taubert et al. 2010; Schlegel et al. 2012).

In the present study, we investigate changes in white matter connectivity as a function of long-term use of sign language compared to spoken language. White matter pathways involved in the processing of acoustic information have been consistently found to be weaker in deaf signers compared to hearing controls, referring to fractional anisotropy (FA), a diffusion MRI (dMRI)-derived quantitative measure of brain microstructure (for a review see Tarabichi et al. 2018). Work focusing on subcortical tracts along the auditory pathway showed that participants with acquired hearing loss exhibit lower FA values in the lateral lemniscus and the inferior colliculus (Lin et al. 2008). Others revealed alterations in cortical white matter tracts such as the right SLF and inferior longitudinal fasciculus, corticospinal tract, inferior fronto-occipital fasciculus, superior occipital fasciculus, and anterior thalamic radiation (Husain et al. 2011). Studies including prelingually and congenitally deaf individuals reported lower FA values in bilateral superior temporal cortex and the splenium of CC in the deaf compared to the hearing group (Li et al. 2012; Karns et al. 2017; Kim et al. 2017). Lower FA points to reduced myelination, lower axonal density, a combination of both, or the presence of crossing fibers in the aforementioned regions, offering a variety of possible interpretations that cannot be construed with certainty (Jones et al. 2013).

The goal of the present study is to go beyond the auditory pathway and resolve the relation between the core language network and its connections to the auditory input and the motor output system necessary for speech processing. To this end, we compared prelingually deaf signers who learned GSL at an early age and could read and write German to a matched hearing control group. We employed dMRI-based probabilistic fiber tractography in order to analyze the connectivity profiles of six major language- and speech-associated areas in both hemispheres. This is a robust and well-established method to study brain connectivity, which provides a measure of the connection probability between a seed region and every voxel in the brain (Behrens et al. 2007). By examining the resulting seed-specific connectivity maps with voxel-based statistics, we were able to compare all connections of a selected region to their full extent and to localize connectivity differences between the two groups. This allowed us to separate speech-specific tracts from pathways of the core language system.

As described above, the core language system responsible for processing semantic and syntactic aspects of language is thought to be distinct from, but to functionally interact with a sensory-motor interface system during the perception and production of speech grounded in white matter pathways (Friederici et al. 2017). We distinguish two types of fibers that are relevant for our study. The first group covers fibers within the core language network, including the dorsally located SLF/AF targeting BA44 and the ventral pathway. The second type includes fibers belonging to the auditory input system as well as fibers belonging to the motor output system. This includes auditory areas and their interhemispheric fibers as well as motor output tracts targeting vBA6.

We anticipated differences in auditory-related white matter pathways involved in speech perception. With respect to the motor output system our expectations for differences were low, since speaking involves muscles similar to those employed in mouthing, an essential part of sign language. Based on the well-documented modality independence of the core language regions (Booth et al. 2002; MacSweeney et al. 2002; Emmorey et al. 2003; Patterson et al. 2007), we expected similar connectivity profiles of the core language pathways connecting BA44 and the posterior temporal cortex. These considerations guided our choice for the selection of seed regions of interest (ROIs) for probabilistic tractography and subsequent analyses. We defined seven ROIs in each hemisphere that served as seed masks for unidirectional probabilistic fiber tracking. These were six language-related ROIs located in BA44, vBA6, IPL, pSTG, pMTG, and HG as well as one control region in the visual cortex. As our goal was to unravel differences and similarities in connections beyond the classic language pathways, we did not define target, waypoint, and exclusion masks in order to compare all possible connections of the specific ROIs.

Materials and Methods

Experimental Design

The present study was designed to investigate the theory which assumes separate neural networks for language and speech. We compared white matter connectivity in hearing and deaf participants. These two groups were chosen, because they display similar language concepts, but communicate differently: exclusively via speech (hearing non-signers) or GSL (deaf signers).

Participants

Fifteen prelingually deaf adults were recruited for the study, but after application of strict inclusion parameters (see below), three among them had to be excluded from further participation. MR-data of 12 prelingually deaf adults who learned GSL within the first years of life and who could read and write German were acquired. Due to uncorrectable motion artifacts in one dataset and an incidental finding in another, only the data of 10 participants (mean age 31 years, range 25–39 years, three men) were analyzed (please see Table 1 for details). All participants were right-handed according to the Edinburgh Handedness Inventory (Oldfield 1971).

Participants of the deaf group had to express a high level of sign language proficiency and use GSL as their primary language of communication. All of them were diagnosed with

Downloaded from https://academic.oup.com/cercor/article-abstract/30/2/812/5543064 by guest on 24 March 2020

Table 1 Demographic data of all deaf participants

Age (y)	Sex	Cause of deafness	Age of onset of hearing impairment (y)	Age of onset of deafness (y;m)	Sign language use from age (y)	Hearing aid	Hearing loss of better ear[a] (dB)	Handedness	Mother/Father deaf
26	F	Unknown	0	2	3	No	94 (left)	Right	No/No
31	F	Rubella during pregnancy	0	0	3	Yes	125 (left)	Right	No/No
25	F	Unknown	0	0;7	6	Yes	109 (right)	Right	No/No
25	F	Unknown	0	0	3	Yes	94 (left)	Right	No/No
27	M	Ototoxic medication	-	1;6	3	No	124 (left)	Right	No/No
33	M	Hereditary	0	0	3	Yes	111 (left)	Right	No/No[b]
37	M	Hereditary	0	0	1	No	111 (left)	Right	Yes/Yes
39	F	Hereditary	0	0	3	No	114 (left)	Right	No/No
33	F	Unknown	0	0	3	No	116 (right)	Right	No/No
31	F	Hereditary	0	0	1	Yes	111 (right)	Right	Yes/Yes

[a]averaged over values at 500 Hz, 1000 Hz, 2000 Hz, and 4000 Hz, [b]Father knows GSL because of deaf grandmother.

sensorineural deafness, were fitted with hearing aids during early childhood and attended schools for deaf students. As there was no newborn hearing screening at the time the participants were born, we grounded our assessment on participants' self-reported history of deafness and other available medical documentation. According to this information, they were either born deaf or with severe progressing hearing impairment (with the exception of one participant who became deaf after receiving ototoxic medication at 1;6 years) so that they experienced deafness before the age of three in all cases. We only included participants with hearing thresholds above 90 dB on the better ear. In addition, their speech was examined by an experienced patholinguist. Those who used speech at a higher level than basic utterances were not included in our study. Pure tone audiometry results are averaged over hearing thresholds at 500 Hz, 1000 Hz, 2000 Hz, and 4000 Hz, because these frequencies best represent the range of spoken language. As 130 dB was the maximum possible stimulation threshold, values of tones that were not heard up to this level were set to 130 dB for averaging.

Ten control subjects (mean age 31 years, range 25–39 years, three men) were matched for sex, age, and handedness and received monetary compensation for their participation. All hearing participants were German native speakers with unremarkable tone audiograms and no knowledge of sign language. No participant reported having a history of neurological disorders or head injuries and all of them had normal neuroanatomy, which was confirmed by a neuroradiologist, who inspected all participants' MR images. After having been informed about risks and procedures, all participants gave written consent. The study was approved by the local Ethics Committee of the Faculty of Medicine at the Technical University of Dresden, and followed the ethical standards of the Helsinki Declaration.

Data Acquisition and Pre-processing of Diffusion Data

Anatomical and diffusion MR images were acquired with a 3 Tesla Tim-Trio MR-tomograph (Siemens Healthineers, Erlangen, Germany; software syngo MR B17) equipped with an eight-channel head coil. After obtaining a high-resolution structural T1-weighted scan, diffusion volumes were acquired with the following parameters: 60 gradient directions with a *b*-value 1000 s/mm^2 and 7 b0-volumes; 63 transversal slices without gap; twice-refocused echo-planar imaging sequence, interleaved recording; field of view 186 × 186 mm; voxel size 1.86 × 1.86 × 1.9 mm; repetition time 11.3 s and echo time 88 ms; 6/8 partial Fourier and GRAPPA 2 acceleration. After visual inspection and verification of absence of artifacts, data were motion corrected using rigid-body transformation computed with FSL (Jenkinson et al. 2002) (University of Oxford, UK, http://www.fmrib.ox.ac.uk/fsl) and linearly registered to the participants' individual T1 anatomy image in one combined step. The aligned diffusion image was masked with the brain mask obtained from the T1 image. Lastly, the diffusion tensor and FA maps were computed in every voxel. For the group analysis, all FA images were eroded and normalized to the FSL-FA template image using a linear and non-linear registration with default parameters (FSL's FLIRT and FNIRT) (Smith et al. 2006).

ROI definition

As depicted in Figure 1, we defined six ROIs in each hemisphere that served as seed masks for probabilistic fiber tracking. To investigate the auditory input system, we placed ROIs in bilateral HG. The ROIs covering the core language network were situated in BA44, pSTG, pMTG, and the central part of the IPL. To examine connections of the pre-motor output system, a ROI was placed in vBA6. Two additional ROIs in left and right primary visual cortex served as seeds for control tracts. The ROIs were drawn manually in ITK-SNAP (Yushkevich et al. 2006) on the FSL-FA-template (isotropic 1 mm resolution) based on anatomical landmarks. In order to separate tracks that start or end in the seed region from tracks that pass through it, we selected only the crown of the respective gyrus (50% of the local sulcal depth) and chose seed voxels at the gray matter/white matter boundary of each ROI in individual space.

The ROI in the pSTG was restricted posteriorly by the temporoparietal junction, superiorly by the Sylvian fissure, inferiorly by the superior temporal sulcus and anteriorly by the posterior border of HG. The latter as a whole was classified as HG ROI. We defined the pMTG ROI parallel to the one in pSTG with the superior temporal sulcus representing its superior border

Downloaded from https://academic.oup.com/cercor/article-abstract/30/2/812/5543064 by guest on 24 March 2020

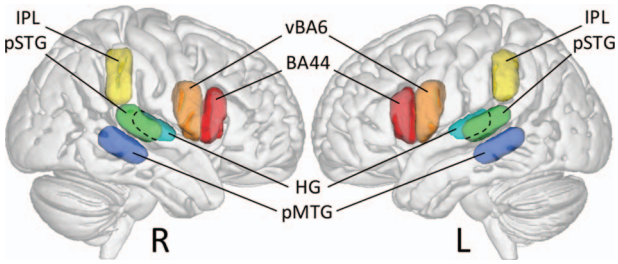

Figure 1. Seed ROIs for probabilistic tractography. Brodmann area 44 (BA44), ventral Brodmann area 6 (vBA6), central part of the IPL, pSTG, pMTG, and HG. HG is situated medial of pSTG and therefore marked with a dashed line. They do not overlap.

and the middle temporal sulcus the inferior one. Medially, all ROIs ended at the transition from gyrus to deep white matter. The ROI in BA44 was drawn over the opercular part of the IFG, with the Sylvian fissure and its anterior ascending ramus forming the inferior and the anterior borders, respectively. It was restricted posteriorly by the precentral sulcus, and its superior boundary was the inferior frontal sulcus. Posteriorly adjacent to BA44, we defined the precentral ROI in vBA6, which reached from the Sylvian fissure up to the IFS and had its posterior border at the central sulcus. The parietal ROI covered the central portion of the IPL posterior to the ascending branch of the Sylvian fissure and was restricted superiorly by the intraparietal sulcus and inferiorly by the temporoparietal junction (Ruschel et al. 2014). The control ROIs in the primary visual cortex were based on the Juelich histological atlas beyond 50% probability (Amunts et al. 2000).

All ROIs were smoothed with a spherical kernel of 2 mm and aligned to each participant's FA images by applying the inverse normalization steps computed in the previous normalization of the individual FA images to the FSL-FA template (Smith et al. 2006). As we intended to start probabilistic tracking at the transition from gray to white matter, the aligned ROIs were masked with participants' individual FA maps at a threshold of 0.15, providing a white matter mask. After removing disconnected voxels left by the masking process, we selected only the white matter border voxels of the resulting ROIs as seed regions. The transition of the FA values between white and gray matter is smooth at the chosen resolution of the diffusion images. An FA threshold of 0.15 provides a white matter mask that might include boundary voxels with a partial volume of gray matter at its borders as revealed by a direct comparison with the segmentation of the high resolution T1 image. This relatively low threshold was chosen to robustly seed the tractography only at the white matter/gray matter boundary. After each step, the ROIs were carefully checked and, if necessary, adjusted to ensure proper alignment. Supplementary Table S1 summarizes the final sizes of all seed ROIs. Note that the applied FA threshold for the seed voxels should not be confused with any threshold applied during the tractography process. Probabilistic tracking was conducted employing a whole brain mask instead of a white matter mask.

Probabilistic Tractography

In preparation for probabilistic tracking, we computed the fiber orientation distribution for every voxel with FSL's BEDPOSTX (Behrens et al. 2007) software. Up to two fiber orientations were modeled in each voxel, which were used for the computation of tracking directions. Probabilistic tracking was performed unidirectionally from each of the 14 seed ROIs separately for every participant. As our goal was to unravel the differences and similarities in connections beyond the classic language pathways and to reduce unequal biases between participants, we did not include any target, waypoint, or exclusion masks. We used FSL PROBTRACKX (Behrens et al. 2007) with default parameters (5000 sample tracts per seed voxel, step length of 0.5 mm, curvature threshold of 0.2, maximum of 2000 steps per streamline, volume fraction threshold of subsidiary fiber orientations of 0.01). As the range of PROBTRACKX output images covered several orders of magnitude, we applied a logarithmic transform to each of the resulting tractography visitation maps to reduce the dynamic range. The transformed maps were then scaled with the log of the total number of streamlines as a function of the seed ROI's size to account for ROI size differences between participants. The resultant individual maps were normalized to the FSL-FA template in MNI space (1 mm isotropic) using the linear and non-linear normalization matrices and maps computed by normalizing the FA images as described before (Smith et al. 2006). The maps were then submitted to voxel-based statistics implemented in SPM12 (Wellcome Trust Centre for Neuroimaging; http://www.fil.ion.ucl.ac.uk/spm).

Apart from the normalization process, which implies a certain degree of smoothing, tractography images were not additionally smoothed. One reason for this approach is that the high resolution FA-based maps used for normalization are less prone to misalignments during registration compared to T1 images, as they provide a sharp white matter definition with high FA values in the centre of each gyrus. Secondly, we were interested in examining focal effects along the pathways. As these can be small in diameter and display some twists and curves along their trajectories, smoothing would erase their fine structure.

Statistical Analysis

The number of computed trajectories per voxel is indicative of the tractography's statistical precision and is influenced by the coherence of the analyzed white matter pathway. This measure relates indirectly to the white matter connectivity of the seed region. We compared the normalized connectivity maps between the two groups of participants to detect areas with reduced connection probability with respect to each seed ROI (Neef et al. 2018). For this statistical analysis, we applied a two-sample t-test (one-tailed) with default parameters in SPM. Areas with low and improbable connectivity values were masked by an explicit mask. For this purpose, we created an average scaled and normalized tractogram of all subjects in MNI-space and masked out regions with values lower than 0.2. For purposes of clarity, we used these average tractograms of all participants for visualization. All results were obtained using an uncorrected *P*-value of 0.005 at voxel level, a family wise error (FWE)-corrected *P*-value of 0.05 at cluster level and a cluster extent threshold of 100 voxels. All contrasts were calculated with $n = 20$.

Post hoc Analyses

Since the absence of a group effect is no evidence for similarity, we calculated interaction effects and Bayes Factor (Nieuwenhuis

Downloaded from https://academic.oup.com/cercor/article-abstract/30/2/812/5543064 by guest on 24 March 2020

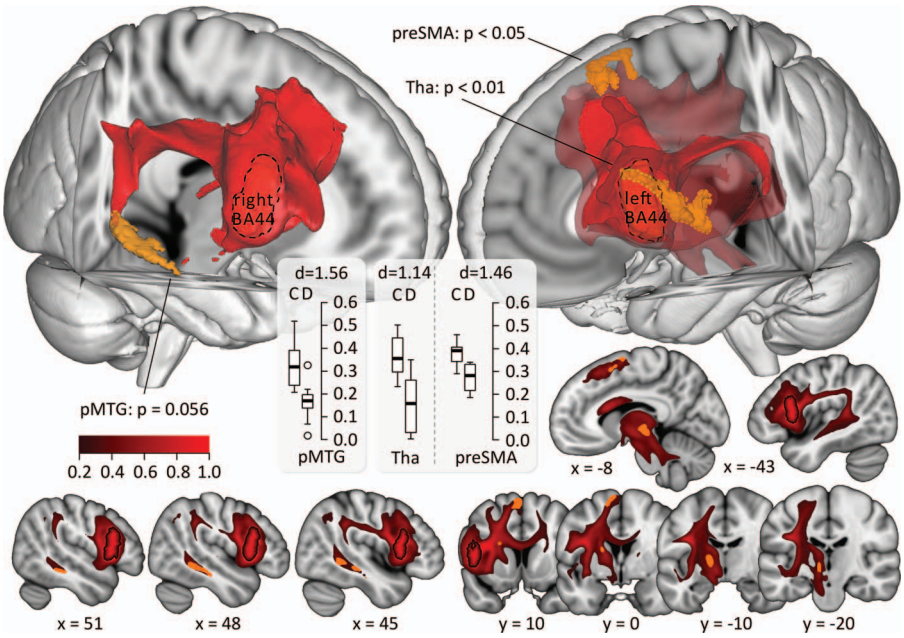

Figure 2. Tractography results with seed in Brodmann area 44 (BA44). Average tractograms of all participants are displayed on the standard T1 MNI-brain. Seed ROIs are marked with dashed lines. Tha, preSMA, and pMTG, where connectivity differed significantly between groups are depicted in orange (pMTG: trend). Color coding in slices ranges from 0 (no connectivity with seed ROI) to 1 (maximal connectivity). Tracts are shown at a threshold of 0.2, which was also used for statistical testing. For purposes of clarity, the tracts in the 3D images are presented at a threshold of 0.3. 3D images and horizontal slices are viewed from above and coronal slices from behind with left in the pictures representing left in the brain. Boxplots indicate mean logarithmized connectivity values of controls (C) and deafs (D) in areas with significant connectivity differences; Cohen's *d* was calculated post hoc. *P*-values are FWE-corrected at cluster level. All coordinates are given in MNI-space.

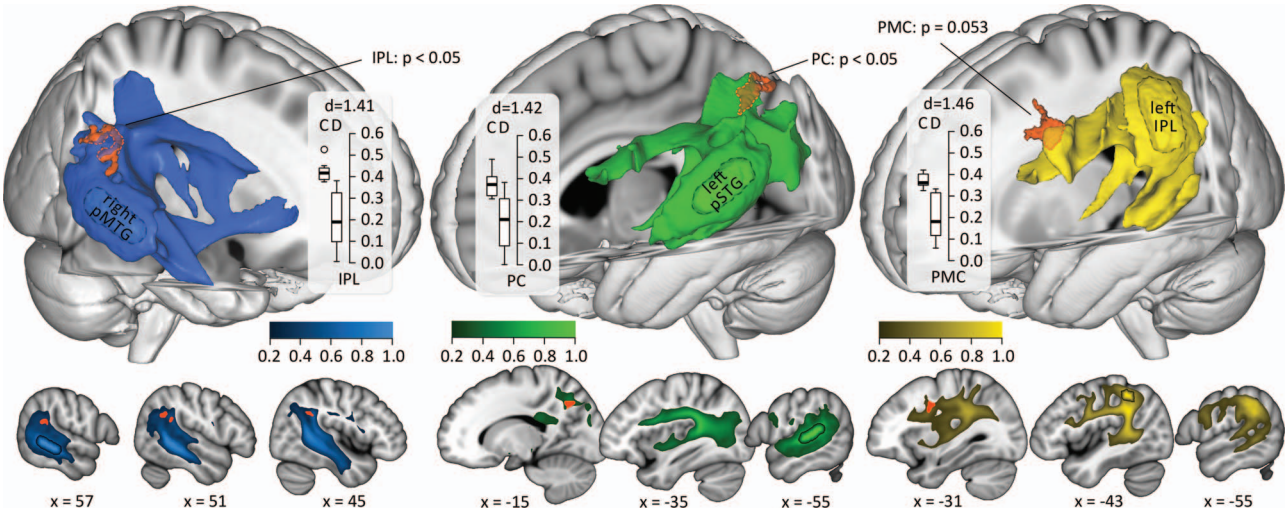

Figure 3. Tractography results with seeds in right pMTG (blue), left pSTG (green) and left IPL (yellow). Average tractograms of all participants are displayed on the standard T1 MNI-brain. Seed ROIs are marked with dashed lines. Right IPL, left precuneus (PC) and left premotor cortex (PMC), where connectivity differed significantly between groups (PMC: trend) are depicted in orange. Color coding in slices ranges from 0 (no connectivity with seed ROI) to 1 (maximal connectivity). Tracts are shown at a threshold of 0.2, which was also used for statistical testing. For purposes of clarity, the tracts in the 3D images are presented at a threshold of 0.3. Sagittal slices show left hemisphere for negative x and right hemisphere for positive x. Boxplots indicate mean logarithmized connectivity values of controls (C) and deafs (D) in areas with significant connectivity differences; Cohen's *d* was calculated post hoc. *P*-values are FWE-corrected at cluster level. All coordinates are given in MNI-space.

et al. 2011; Wetzels et al. 2011) in R (R Core Team 2016) for two tracts: the FAT representing the speech production network and the AF as part of the core language network. To this end, we selected the significant region in the left preSMA (please see results) and defined a similar region in the left posterior temporal cortex by defining a sphere around the two original seed ROIs in pMTG and pSTG. We chose these two regions in order to directly compare AF and FAT with respect to their targets when starting tractography in BA44. We masked the original connectivity maps with a mean map of all participants at a threshold of 0.2 to exclude improbable results. Within this map we extracted mean connectivity values for the significant region in the preSMA and for the previously defined region in the posterior temporal cortex. Calculation method and

Downloaded from https://academic.oup.com/cercor/article-abstract/30/2/812/5543064 by guest on 24 March 2020

Table 2 Results of probabilistic tractography

Seed	Connectivity difference in	Cluster size	Cluster p (FWE-corrected)	Peak T	Peakcoordinates (mm) x	y	z	Mean connectivity controls	deaf	Effect size (Cohen's *d*)
Left BA44	Left preSMA	673	0.024	4.36	−2	10	65	0.37	0.16	1.46
Left BA44	Left Tha	1001	0.003	4.11	−16	−4	14	0.38	0.28	1.14
Right BA44	Right MTG	490	0.056	4.93	47	−40	−7	0.33	0.16	1.56
Left HG	CC	2296	0.000	4.39	5	−31	17	0.38	0.18	1.38
Left HG	Left precuneus	671	0.013	4.39	−19	−60	37	0.47	0.25	1.27
Right HG	CC	1146	0.000	5.73	−18	−33	38	0.37	0.16	1.50
Left IPL	Left PMC	368	0.053	4.66	−30	−2	38	0.37	0.19	1.46
Left pSTG	Left precuneus	422	0.037	4.49	−14	−66	41	0.37	0.20	1.42
Right pMTG	Right IPL	539	0.023	4.47	45	−46	30	0.42	0.21	1.41

Note: HG: Heschl's gyrus; IPL: inferior parietal lobule; pSTG/pMTG: posterior superior/middle temporal gyrus; preSMA: pre-supplementary motor area; PMC: premotor cortex

nomenclature for the Bayes Factor are taken from the paper by Wetzels et al. (2011).

Data Availability

In alignment with the data protection clause in the ethics protocol which governed this study, data are available in non-identifiable format upon request. All analyses were conducted in FSL and SPM and are described above. No custom algorithms were used for analysis.

Results

Core Language Network

We reliably found the SLF/AF in both groups, confirming that our ROIs were placed appropriately. The different components of this pathway could be tracked bilaterally in both directions seeding frontally in BA44 (Fig. 2) and vBA6 (see Supplementary Fig. S1) as well as temporally in pMTG and pSTG (Fig. 3 and Supplementary Fig. S2). We detected no significant group differences for these fiber tracts. The IPL ROIs (Fig. 3 and Supplementary Fig. S2) also connected to frontal and temporal cortices via the short segments of the SLF/AF (Catani et al. 2005) in both hemispheres. This core pathway of the language network in the left hemisphere was not affected by early deafness and appeared to be similar in both groups. The ventral connections of the posterior temporal and the IPL ROIs towards the frontal lobe (Fig. 3 and Supplementary Fig. S2) did not display significant group differences.

Speech Perception and Production Network

We detected a number of pathways with significantly lower connection probability in the deaf group compared to the control group. These tracts are associated not with language processing in general, but with the production and perception of speech in particular. The differences in connectivity spanned a volume of at least 100 adjacent voxels at an FWE $P < 0.05$, corrected at cluster level. Pathways and regions with significant connectivity differences were smoothed for display in the sliced MR images. Effect sizes were calculated based on connectivity values in those regions with significant connectivity differences and were plotted with the corresponding MR images in standard space (Figs 2–4). Supplementary Tables S2–S8 provide a full list of results.

Speech Perception

The most striking group differences in the speech perception network appeared in the tracts seeded in bilateral HG, where both transcallosal connections (left-to-right and right-to-left) had significantly lower connectivity values in the deaf than in the control group (left: $P < 0.001$, right: $P < 0.001$; for details see Fig. 4 and Table 2). With regard to the left HG, the deaf group further showed a weaker continuation of the transcallosal connection towards the contralateral parietal and posterior temporal cortices. Moreover, the connections of the left HG (Fig. 4; $P = 0.01$) and the left pSTG (Fig. 3; $P < 0.05$) towards the ipsilateral PC had significantly lower probabilities in the deaf group, similar to the tract between the right pMTG and the right IPL (Fig. 3; $P < 0.05$).

Speech Production

Concerning speech production, tractography revealed significantly lower connectivity values for the left Broca–Tha–preSMA loop in the deaf group (Fig. 2; BA44 to preSMA: $P < 0.05$, BA44 to Tha: $P < 0.005$). Though only apparent as a trend ($P = 0.053$), the left IPL and the left PMC had a lower connection probability in the deaf than in the hearing group, strengthening this finding (Fig. 3). With regard to the right BA44 as seed ROI, we observed a trend to lower connectivity with the ipsilateral pMTG in the deaf group (Fig. 2; $P = 0.056$).

In order to test for a dissociation of a core language network and an output system for speech processing, we directly compared AF and FAT with respect to their targets when starting tractography in BA44 (Fig. 5). A repeated measures ANOVA with the between-groups factor "hearing status" and the within-groups factor "tract" revealed a significant interaction between "hearing status" and "tract" ($F_{1,36} = 11.471$, $P = 0.0017$) and a significant main effect of "hearing status" ($F_{1,36} = 13.232$, $P = 0.0009$). There was no main effect of the factor "tract" ($F_{1,36} = 0.431$, $P = 0.52$). Pairwise post hoc comparisons (corrected for multiple comparisons; Holm 1979) showed that the main effect "hearing status" was driven by the group difference in the FAT ($P = 0.0013$, one-tailed), while the groups' means did not differ in the AF ($P = 0.41$, one-tailed). These findings were corroborated by their respective Bayes Factor. We found very strong evidence for the group difference in the FAT ($BF_{A0} = 59.39$). The Bayes Factor for the AF was $BF_{0A} = 3.17$, providing substantial evidence for similarity. Additionally, we reconstructed control tracts from visual seed ROIs and found similar trajectories in both groups without significant differences.

Downloaded from https://academic.oup.com/cercor/article-abstract/30/2/812/5543064 by guest on 24 March 2020

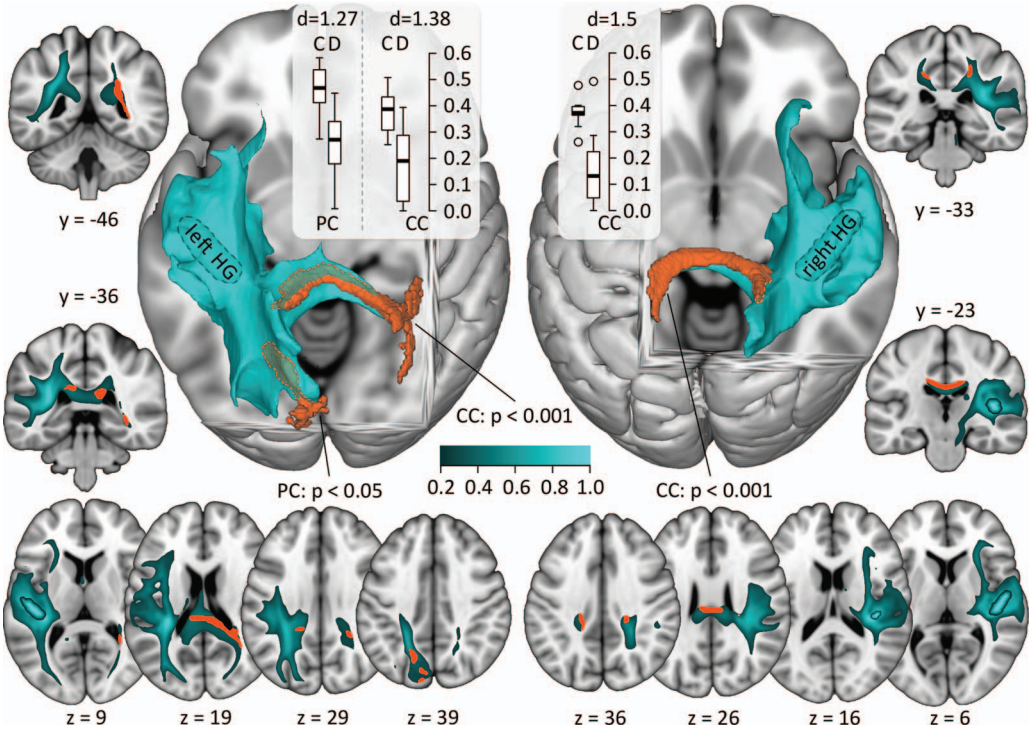

Figure 4. Tractography results with seed in HG. Average tractograms of all participants are displayed on the standard T1 MNI-brain. Seed ROIs are marked with dashed lines. CC and left PC, where connectivity differed significantly between groups are depicted in orange. Color coding in slices ranges from 0 (no connectivity with seed ROI) to 1 (maximal connectivity). Tracts are shown at a threshold of 0.2, which was also used for statistical testing. For purposes of clarity, the tracts in the 3D images are presented at a threshold of 0.3. 3D images and horizontal slices are viewed from above and coronal slices from behind with left in the pictures representing left in the brain. Boxplots indicate mean logarithmized connectivity values of controls (C) and deafs (D) in areas with significant connectivity differences; Cohen's *d* was calculated post hoc. *P*-values are FWE-corrected at cluster level. All coordinates are given in MNI-space.

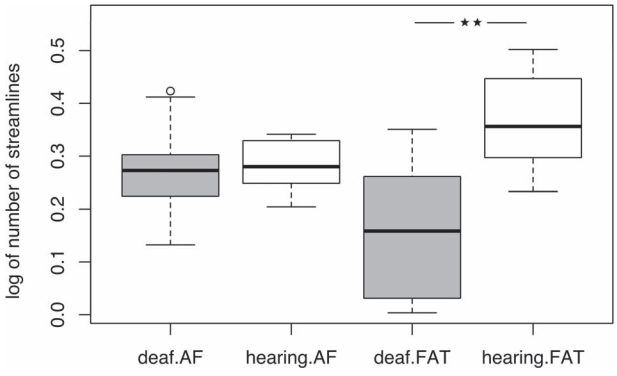

Figure 5. Connectivity values in the left FAT seeded in BA44 and targeting the preSMA and the left AF seeded in BA44 and targeting posterior temporal cortex. Boxplots indicate mean logarithmized connectivity values of deaf (gray) and hearing (white) participants in AF and FAT with a significant group difference in the FAT ($P = 0.0013$, one-tailed) and no significant group difference in the AF ($P = 0.41$, one-tailed). *P*-values are corrected for multiple comparisons. Asterisk indicates significance at $^{**}P < 0.01$.

Discussion

Using a novel approach for analyzing probabilistic tractography group differences, we were able to disentangle white matter pathways involved in speech processing from those subserving language itself. This finding provides structural evidence for the theoretically-proposed segregation of a core language system and input/output systems responsible for externalization (Friederici et al. 2017). We reliably found the major dorsal language tract, which is the SLF/AF targeting BA44, in both groups, underlining the general modality-independence of the core language network (MacSweeney et al. 2002), further supported by similar connection probabilities in the ventral language pathway of both deaf and hearing participants. In contrast, regions of the sensory-motor system involved in the production and perception of speech had significantly lower connectivity values in the deaf group compared to the hearing group, indicating their modality dependency. Moreover, producing and understanding spoken language is claimed to rely on fast feedback mechanisms between the core language network and the speech network, including the (sub)cortical motor system, oropharyngeal muscles and the hearing system (Dick et al. 2014). In prelingually deaf individuals, these input/output related circuits do not seem to be equally well established. The present results call for a fine-grained discussion of BA44 region's role in the core language system and its relation to the sensory-motor system, including subcortical parts of the production networks. Before doing so we will consider the perception network involving the left and the right hemisphere.

Concerning circuits subserving speech perception, there exists a general scientific consensus with regard to the identification of degraded subcortical auditory pathways in deaf individuals (Lin et al. 2008; Tarabichi et al. 2018). In this study, we built on previous results (Li et al. 2012) by showing that the callosal connection between the auditory cortices appears to

Downloaded from https://academic.oup.com/cercor/article-abstract/30/2/812/5543064 by guest on 24 March 2020

be weakened in prelingually deaf individuals. This connection seems to be crucial for a rapid transfer of acoustic information processed in both hemispheres at an early cortical processing stage, as indicated by white matter changes in the splenial CC of professional interpreters (Elmer et al. 2011). They rely on the fast integration of interhemispheric computational differences (Hickok and Poeppel 2007) with the left auditory cortex being more responsive to high-temporal (segmental) changes in speech signals and the right one to spectral (supra-segmental) variations (Zatorre and Belin 2001). Furthermore, our analyses yielded lower connectivity between the left HG and contralateral parietal as well as midtemporal cortices. This connection provides a structural basis for the interhemispheric interaction needed for sentence-level auditory prosody processing with a commissural connection that directly links the primary auditory cortex to contralateral higher-order integration areas (Friederici et al. 2007). The identification of less developed pathways for auditory prosody processing in our study's deaf participants was complemented by lower connection probabilities between the right MTG seed and the IPL as well as between the right BA44 seed and the MTG. This finding underlines the role of these tracts in the processing of speech (Price 2012).

Apart from transferring prosodic speech information (Friederici et al. 2007), the splenium of the CC is known to be crucial for attention-demanding tasks in the auditory, visual, and tactile domains with the right hemisphere outperforming the left one (Dimond 1979). The missing auditory attention capacities of the deaf group may have further contributed to the reduced transcallosal connectivity of the auditory cortices. Although some auditory features such as tonotopic functional connectivity seem to be preserved to varying degrees in severely hearing-impaired individuals (Striem-Amit et al. 2016), the connections described above might not be completely established in such individuals. They may be diminished due to pruning processes in early childhood occurring in the context of auditory deprivation and/or due to the later lack of use.

Deafness is not only about hearing and speech perception, but also about producing speech. The neural network that is responsible for speech production encompasses motor as well as somatosensory and auditory regions involved in feedback loops for real-time adjustment of articulatory output (Price 2012). One of the tracts that seems to be associated with producing fluent speech is the FAT between left BA44/vBA6 and preSMA/SMA, two regions crucial for speech initiation (Price 2012; Catani et al. 2013; Flinker et al. 2015). As the deaf participants in our study hardly communicate orally, this pathway may not have developed to its fullest possible extent. In the group comparisons of the BA44 connectivity profiles, the respective values of the FAT were lower in the deaf group, which highlights its importance for speech initiation and builds on the findings from a post-stroke aphasia study demonstrating FAT involvement in speech fluency (Halai et al. 2017).

The connection between the left BA44 and the Tha as part of the cortico-basal ganglia-thalamo-cortical circuit for motor processing of speech (Dick et al. 2014) also showed reduced connection probability in the deaf group. This is in line with previous results (Lyness et al. 2014) and underlines our finding of weakened connections involved in speech production, owing to this projection's role in supporting phonological language processing. We argue in favor of this suggestion based on deaf signers' limited capability of auditory phonological processing. There is phonology in sign language, but note that it is based upon hand configuration, location and movement (Sandler 2012).

The present findings illustrates BA44's key role as integration node in the language and speech network. It covers syntactic processing via the SLF/AF between BA44 and the posterior temporal cortex (Friederici et al. 2006; Skeide et al. 2016) independent of modality, reflected in the two groups' similar SLF/AF connectivity profiles. Moreover, it plays a crucial part in speech planning and initiation. In this role, however, BA44 reveals lower connectivity values in the tracts towards the preSMA and the Tha in the deaf group. As described above, vBA6 is functionally distinct from BA44 (Flinker et al. 2015) and covers those regions in the precentral gyrus which are relevant for mouth and facial movements—crucial in sign language. As such, the two groups' similar connectivity profiles with regard to vBA6 may be explained by this region's relevance for both speaking and mouthing during signing.

The PMC has been implicated in auditory discrimination of speech sounds as well as in auditory-motor mapping of speech and is involved in speech repetition, articulation and phonological word learning (Price 2012; López-Barroso et al. 2013; Flinker et al. 2015). These functions strongly rely on one part of the SLF/AF, which connects temporoparietal regions to the PMC as part of the dorsal pathway (Saur et al. 2008). While we observed no differences in the long segment of this pathway connecting the left temporal seed ROIs and BA44 known to be relevant for syntactic processes, the SLF's connectivity values between the left IPL seed and PMC were lower in the deaf group, emphasizing this part's role in auditory-motor integration during speech processing.

The connection between left supramarginal gyrus and PMC represents a key component of audiovisual speech processing that matures as experience in producing and perceiving spoken language increases (Dick et al. 2010). The lower connection probabilities we found in the deaf group are consistent with this model, because perceptional and articulatory deficits prevent audiovisual integration and further development of the respective pathways. As shown in an audiovisual fusion study, these pathways do not regrow after successful restoration of hearing with a cochlear implant (Schorr et al. 2005). Our results provide neuroanatomical underpinnings for these findings. In addition to this frontoparietal connection, the connectivity values between the left HG/pSTG seed and the ipsilateral PC extending to the intraparietal and parieto-occipital sulcus were significantly lower in the deaf group. These regions have been suggested to contribute to auditory-visual object recognition (for a review see Price 2012), completing the picture of a diminished fronto-temporo-parietal circuit for spoken language in the deaf group.

In order to obtain the results discussed above, we used probabilistic tractography. There are some methodological considerations concerning this technique. As it is an indirect measure of brain microstructure and connectivity, exact conclusions concerning the causes of the observed effects, such as changes in axonal diameter, myelinization, and fiber density cannot be drawn. Based on this indirect relation, connection probability is only a relative measure for actual connectivity. In this context, connectivity values serve as a correlate that can be compared between groups. Furthermore, dMRI is susceptible to measurement errors that may lead to the indication of inexistent connections or the negation of existing ones. It is important to note that, owing to sensitivity differences between the voxels close to a seed ROI and those voxels further away

Downloaded from https://academic.oup.com/cercor/article-abstract/30/2/812/5543064 by guest on 24 March 2020

from it, some connections may be detected in one tracking direction, but remain unidentifiable in the reverse one. We observed this effect in three regions: the left PMC, the left IPL, and the right MTG (Jones et al. 2013). Another methodological aspect to consider when interpreting the results is the limited sample size. This reduces the study's power and might have contributed to the absence of effects in some contrasts of our study. Here, further research with larger samples is needed in order to confirm and extend our results. However, taking into account existing fMRI research, strict selection procedures for participation in the current study, careful inspection of the data at all stages and the use of complex crossing fiber models (Behrens et al. 2007), we are confident that our results represent an important contribution to our understanding of the neural networks for speech and language.

Our findings of a preserved core language network paired with weaker tracts for speech processing in prelingually deaf signers certainly raise several issues. When studying deaf signing populations without a hearing signing control sample, it is not possible to clearly separate effects caused by auditory deprivation from those related to sign language use. Although we cannot directly compare our results to those of hearing signers, we interpret the observed effects in the context of auditory deprivation nevertheless. The reason for this is twofold. First, missing auditory input has a direct impact on the interhemispheric connections between the primary auditory areas, and this effect presumably occurs independently of sign language use. Second, all significant effects were reductions in the deaf group, pointing to tracts weakened by relatively low or no use. In the case of the pathways connecting the core language network with the sensory-motor system, the effects may be attributed to the absence of oral communication. This, in turn, is related to deafness and the lack of auditory feedback during speaking, but not to the use of sign language. Importantly, however, we ascribe the absence of connectivity differences in the core language pathways to early acquisition and use of sign language. These pathways appear to be equally developed in the deaf group, corroborating the concept of modality-independence of the core language network. Our study does not allow for conclusions about differential effects of early-onset as opposed to long-lasting deafness. Here, further research comparing prelingually deaf adults to long-term postlingually deaf participants is needed in order to disentangle developmental effects from the deterioration of pathways caused by long-lasting deafness.

Here, we showed that prelingual deafness paired with the early acquisition of sign language does not seem to affect the core language pathways, but may lead to changes in the connectivity of sensory and motor planning areas necessary for the processing of spoken language. The core language network seems to mature as long as either auditory or visual language input is provided in early childhood. In contrast, the pathways necessary for speech processing explicitly need auditory input and active speaking in order to mature to their full extent. Taken together, our findings demonstrate the modality-independence of the language network and provide structural evidence for the segregation of the core language system and speech processing circuits.

Supplementary Material

Supplementary material is available at *Cerebral Cortex* online.

Funding

German Research Foundation (grant number DFG/Ha 3153/2-1).

Note

We thank Alexander Mainka, Katrin Palisch and Stephan Schoebel for helping us with the recruitment of participants and we thank Steffi Heinemann for supporting the classification of the deaf participants' speech capacities.

Author's Contributions

AA, AH, ADF, DM, and JG designed the study; TF performed the research; TF and AA analyzed the data; TF, AA, AH and ADF wrote the paper.

References

Amunts K, Malikovic A, Mohlberg H, Schormann T, Zilles K. 2000. Brodmann's areas 17 and 18 brought into stereotaxic space—where and how variable? *NeuroImage*. 11:66–84.

Anwander A, Tittgemeyer M, von Cramon DY, Friederici AD, Knösche TR. 2007. Connectivity-based parcellation of Broca's area. *Cereb Cortex*. 17:816–825.

Bajada CJ, Lambon Ralph MA, Cloutman LL. 2015. Transport for language south of the Sylvian fissure: the routes and history of the main tracts and stations in the ventral language network. *Cortex*. 69:141–151.

Behrens TEJ, Berg HJ, Jbabdi S, Rushworth MFS, Woolrich MW. 2007. Probabilistic diffusion tractography with multiple fibre orientations: what can we gain? *NeuroImage*. 34:144–155.

Berwick RC, Friederici AD, Chomsky N, Bolhuis JJ. 2013. Evolution, brain, and the nature of language. *Trends Cogn Sci*. 17:89–98.

Booth JR, Burman DD, Meyer JR, Gitelman DR, Parrish TB, Mesulam MM. 2002. Modality independence of word comprehension. *Hum Brain Mapp*. 16:251–261.

Brauer J, Anwander A, Friederici AD. 2011. Neuroanatomical prerequisites for language functions in the maturing brain. *Cereb Cortex*. 21:459–466.

Catani M, Jones DK, Ffytche DH. 2005. Perisylvian language networks of the human brain. *Ann Neurol*. 57:8–16.

Catani M, Mesulam MM, Jakobsen E, Malik F, Martersteck A, Wieneke C, Thompson CK, Thiebaut de Schotten M, Dell'Acqua F, Weintraub S *et al*. 2013. A novel frontal pathway underlies verbal fluency in primary progressive aphasia. *Brain*. 136:2619–2628.

Chao Y-P, Cho K-H, Yeh C-H, Chou K-H, Chen J-H, Lin C-P. 2009. Probabilistic topography of human corpus callosum using cytoarchitectural parcellation and high angular resolution diffusion imaging tractography. *Hum Brain Mapp*. 30:3172–3187.

Dick AS, Bernal B, Tremblay P. 2014. The language connectome: new pathways, new concepts. *The Neuroscientist*. 20:453–467.

Dick AS, Garic D, Graziano P, Tremblay P. 2019. The frontal aslant tract (FAT) and its role in speech, language and executive function. *Cortex*. 111:148–163.

Dick AS, Solodkin A, Small SL. 2010. Neural development of networks for audiovisual speech comprehension. *Brain Lang*. 114:101–114.

Dimond SJ. 1979. Tactual and auditory vigilance in split-brain man. *J Neurol Neurosurg Psychiatry*. 42:70–74.

Draganski B, Gaser C, Busch V, Schuierer G, Bogdahn U, May A. 2004. Neuroplasticity: changes in gray matter induced by training. *Nature*. 427:311–312.

Downloaded from https://academic.oup.com/cercor/article-abstract/30/2/812/5543064 by guest on 24 March 2020

Elmer S, Hänggi J, Meyer M, Jäncke L. 2011. Differential language expertise related to white matter architecture in regions subserving sensory-motor coupling, articulation, and interhemispheric transfer. *Hum Brain Mapp*. 32:2064–2074.

Emmorey K, Allen JS, Bruss J, Schenker N, Damasio H. 2003. A morphometric analysis of auditory brain regions in congenitally deaf adults. *Proc Natl Acad Sci*. 100:10049–10054.

Finney EM, Fine I, Dobkins KR. 2001. Visual stimuli activate auditory cortex in the deaf. *Nat Neurosci*. 4:1171–1173.

Flinker A, Korzeniewska A, Shestyuk AY, Franaszczuk PJ, Dronkers NF, Knight RT, Crone NE. 2015. Redefining the role of Broca's area in speech. *Proc Natl Acad Sci*. 112:2871–2875.

Friederici AD, Bahlmann J, Heim S, Schubotz RI, Anwander A. 2006. The brain differentiates human and non-human grammars: functional localization and structural connectivity. *Proc Natl Acad Sci U S A*. 103:2458–2463.

Friederici AD, Chomsky N, Berwick RC, Moro A, Bolhuis JJ. 2017. Language, mind and brain. *Nat Hum Behav*. 1:713–722.

Friederici AD, von Cramon DY, Kotz SA. 2007. Role of the corpus callosum in speech comprehension: interfacing syntax and prosody. *Neuron*. 53:135–145.

Halai AD, Woollams AM, Lambon Ralph MA. 2017. Using principal component analysis to capture individual differences within a unified neuropsychological model of chronic post-stroke aphasia: revealing the unique neural correlates of speech fluency, phonology and semantics. *Cortex*. 86: 275–289.

Hagoort P, Indefrey P. 2014. The neurobiology of language beyond single words. *Annu Rev Neurosci*. 37:347–362.

Harris M, Beech JR. 1998. Implicit phonological awareness and early reading development in prelingually deaf children. *J Deaf Stud Deaf Educ*. 3:205–216.

Hickok G, Poeppel D. 2007. The cortical organization of speech processing. *Nat Rev Neurosci*. 8:393–402.

Holm S. 1979. A simple sequentially rejective multiple test procedure. *Scand J Stat*. 6:65–70.

Huang H, Zhang J, Jiang H, Wakana S, Poetscher L, Miller MI, van Zijl PC, Hillis AE, Wytik R, Mori S. 2005. DTI tractography based parcellation of white matter: application to the mid-sagittal morphology of corpus callosum. *NeuroImage*. 26:195–205.

Husain FT, Medina RE, Davis CW, Szymko-Bennett Y, Simonyan K, Pajor NM, Horwitz B. 2011. Neuroanatomical changes due to hearing loss and chronic tinnitus: a combined VBM and DTI study. *Brain Res*. 1369:74–88.

Jenkinson M, Bannister P, Brady M, Smith S. 2002. Improved optimization for the robust and accurate linear registration and motion correction of brain images. *NeuroImage*. 17:825–841.

Jones DK, Knösche TR, Turner R. 2013. White matter integrity, fiber count, and other fallacies: the do's and don'ts of diffusion MRI. *NeuroImage*. 73:239–254.

Karns CM, Stevens C, Dow MW, Schorr EM, Neville HJ. 2017. Atypical white-matter microstructure in congenitally deaf adults: a region of interest and tractography study using diffusion-tensor imaging. *Hear Res*. 343:72–82.

Kim J, Choi JY, Eo J, Park H-J. 2017. Comparative evaluation of the white matter fiber integrity in patients with prelingual and postlingual deafness. *NeuroReport*. 28:1103.

Leonard MK, Ramirez NF, Torres C, Travis KE, Hatrak M, Mayberry RI, Halgren E. 2012. Signed words in the congenitally deaf evoke typical late lexicosemantic responses with no early visual responses in left superior temporal cortex. *J Neurosci*. 32:9700–9705.

Li Y, Ding G, Booth JR, Huang R, Lv Y, Zang Y, He Y, Peng D. 2012. Sensitive period for white-matter connectivity of superior temporal cortex in deaf people. *Hum Brain Mapp*. 33: 349–359.

Lillo-Martin DC, Gajewski J. 2014. One grammar or two? Sign languages and the nature of human language. *Wiley Interdiscip Rev Cogn Sci*. 5:387–401.

Lin Y, Wang J, Wu C, Wai Y, Yu J, Ng S. 2008. Diffusion tensor imaging of the auditory pathway in sensorineural hearing loss: changes in radial diffusivity and diffusion anisotropy. *J Magn Reson Imaging*. 28:598–603.

López-Barroso D, Catani M, Ripollés P, Dell'Acqua F, Rodríguez-Fornells A, de Diego-Balaguer R. 2013. Word learning is mediated by the left arcuate fasciculus. *Proc Natl Acad Sci U S A*. 110:13168–13173.

Lyness RC, Alvarez I, Sereno MI, MacSweeney M. 2014. Microstructural differences in the thalamus and thalamic radiations in the congenitally deaf. *NeuroImage*. 100:347–357.

MacSweeney M, Woll B, Campbell R, McGuire PK, David AS, Williams SCR, Suckling J, Calvert GA, Brammer MJ. 2002. Neural systems underlying British Sign Language and audio–visual English processing in native users. *Brain*. 125:1583–1593.

Neef NE, Anwander A, Bütfering C, Schmidt-Samoa C, Friederici AD, Paulus W, Sommer M. 2018. Structural connectivity of right frontal hyperactive areas scales with stuttering severity. *Brain*. 141:191–204.

Nieuwenhuis S, Forstmann BU, Wagenmakers E-J. 2011. Erroneous analyses of interactions in neuroscience: a problem of significance. *Nat Neurosci*. 14:1105–1107.

Oldfield RC. 1971. The assessment and analysis of handedness: the Edinburgh inventory. *Neuropsychologia*. 9:97–113.

Patterson K, Nestor PJ, Rogers TT. 2007. Where do you know what you know? The representation of semantic knowledge in the human brain. *Nat Rev Neurosci*. 8:976–987.

Perani D, Saccuman MC, Scifo P, Anwander A, Spada D, Baldoli C, Poloniato A, Lohmann G, Friederici AD. 2011. Neural language networks at birth. *Proc Natl Acad Sci U S A*. 108: 16056–16061.

Petacchi A, Laird AR, Fox PT, Bower JM. 2005. Cerebellum and auditory function: an ALE meta-analysis of functional neuroimaging studies. *Hum Brain Mapp*. 25:118–128.

Price CJ. 2012. A review and synthesis of the first 20 years of PET and fMRI studies of heard speech, spoken language and reading. *NeuroImage*. 62:816–847.

R Core Team. 2016. *R: a language and environment for statistical computing*. R Foundation for Statistical Computing.

Ruschel M, Knösche TR, Friederici AD, Turner R, Geyer S, Anwander A. 2014. Connectivity architecture and subdivision of the human inferior parietal cortex revealed by diffusion MRI. *Cereb Cortex*. 24:2436–2448.

Sammler D, Grosbras M-H, Anwander A, Bestelmeyer PEG, Belin P. 2015. Dorsal and ventral pathways for prosody. *Curr Biol*. 25:3079–3085.

Sammler D, Cunitz K, Gierhan SM, Anwander A, Adermann J, Meixensberger J, Friederici AD. 2018. White matter pathways for prosodic structure building: a case study. *Brain Lang*. 183:1–10.

Sandler W. 2012. The phonological organization of sign languages. *Lang Linguist Compass*. 6:162–182.

Saur D, Kreher BW, Schnell S, Kümmerer D, Kellmeyer P, Vry M-S, Umarova R, Musso M, Glauche V, Abel S *et al*. 2008.

Downloaded from https://academic.oup.com/cercor/article-abstract/30/2/812/5543064 by guest on 24 March 2020

Ventral and dorsal pathways for language. *Proc Natl Acad Sci*. 105:18035–18040.

Schlegel AA, Rudelson JJ, Tse PU. 2012. White matter structure changes as adults learn a second language. *J Cogn Neurosci*. 24:1664–1670.

Schorr EA, Fox NA, van Wassenhove V, Knudsen EI. 2005. Auditory-visual fusion in speech perception in children with cochlear implants. *Proc Natl Acad Sci U S A*. 102:18748–18750.

Skeide MA, Brauer J, Friederici AD. 2016. Brain functional and structural predictors of language performance. *Cereb Cortex*. 26:2127–2139.

Smith RJ, Shearer AE, Hildebrand MS, Van Camp G. 1993. Deafness and hereditary hearing loss overview. In: Pagon RA, Adam MP, Ardinger HH, Wallace SE, Amemiya A, Bean LJ, Bird TD, Fong C-T, Mefford HC, Smith RJ, Stephens K, editors. *GeneReviews®*. Seattle (WA): University of Washington, Seattle.

Smith SM, Jenkinson M, Johansen-Berg H, Rueckert D, Nichols TE, Mackay CE, Watkins KE, Ciccarelli O, Cader MZ, Matthews PM *et al*. 2006. Tract-based spatial statistics: voxelwise analysis of multi-subject diffusion data. *NeuroImage*. 31:1487–1505.

Striem-Amit E, Almeida J, Belledonne M, Chen Q, Fang Y, Han Z, Caramazza A, Bi Y. 2016. Topographical functional connectivity patterns exist in the congenitally, prelingually deaf. *Sci Rep*. 6:29375.

Tarabichi O, Kozin ED, Kanumuri VV, Barber S, Ghosh S, Sitek KR, Reinshagen K, Herrmann B, Remenschneider AK, Lee DJ. 2018. Diffusion tensor imaging of central auditory pathways in patients with sensorineural hearing loss: a systematic review. *Otolaryngol Head Neck Surg*. 158: 432–442.

Taubert M, Draganski B, Anwander A, Müller K, Horstmann A, Villringer A, Ragert P. 2010. Dynamic properties of human brain structure: learning-related changes in cortical areas and associated fiber connections. *J Neurosci*. 30: 11670–11677.

Upadhyay J, Hallock K, Ducros M, Kim D-S, Ronen I. 2008. Diffusion tensor spectroscopy and imaging of the arcuate fasciculus. *NeuroImage*. 39:1–9.

Wetzels R, Matzke D, Lee MD, Rouder JN, Iverson GJ, Wagenmakers E-J. 2011. Statistical evidence in experimental psychology: an empirical comparison using 855 t tests. *Perspect Psychol Sci*. 6:291–298.

Yushkevich PA, Piven J, Hazlett HC, Smith RG, Ho S, Gee JC, Gerig G. 2006. User-guided 3D active contour segmentation of anatomical structures: significantly improved efficiency and reliability. *NeuroImage*. 31:1116–1128.

Zatorre RJ, Belin P. 2001. Spectral and temporal processing in human auditory cortex. *Cereb Cortex*. 11:946–953.

Zatorre RJ, Mondor TA, Evans AC. 1999. Auditory attention to space and frequency activates similar cerebral systems. *NeuroImage*. 10:544–554.

Zhang Y, Fan L, Caspers S, Heim S, Song M, Liu C, Mo Y, Eickhoff SB, Amunts K, Jiang T. 2017. Cross-cultural consistency and diversity in intrinsic functional organization of Broca's region. *NeuroImage*. 150:177–190.

Downloaded from https://academic.oup.com/cercor/article-abstract/30/2/812/5543064 by guest on 24 March 2020